PCCP

PAPER

View Article Online
View Journal | View Issue

Cite this: *Phys. Chem. Chem. Phys.*, 2025, **27**, 17557

Emission of velocity correlated clusters up to Ag_{21}^+ induced by keV C_{60}^- impacting a silver surface

E. Armon, A. Bekkerman, B. Tsipinyuk and E. Kolodney *

Received 3rd June 2025,
Accepted 27th July 2025

DOI: 10.1039/d5cp02092a

rsc.li/pccp

Earlier measurements of the velocity correlated cluster emission (VCCE) effect in keV C_{60}^- impact with a silver target (Ag_n^+ (n = 1–9), E. Armon, A. Bekkerman, Y. Cohen, J. Bernstein, B. Tsipinyuk, E. Kolodney, *Phys. Rev. Lett.*, 2014, **113**, 027604) are extended to much larger clusters up to Ag_{21}^+. This is the largest range of cluster size demonstrated so far for the impact induced emission of velocity correlated clusters from any target. Measurements of the kinetic energy distributions (KEDs) of all emitted Ag_n^+ (n = 1–21) cluster ions showed that the VCCE effect as exhibited by a linear increase of most probable energies of the KEDs as a function of cluster size, $E_{mp}(n)$ is still valid up to Ag_{21}^+. The extension of the cluster size range was achieved mainly by applying a higher extraction/acceleration voltage for the surface emitted cluster ions than done before for the smaller range ($U_{ext.}$ = 100 V as compared with 25 V before). The preferential collection and detection of some off-normal lower energy cluster ions resulted in a rather moderate and nearly constant 1–2 eV decrease of $E_{mp}(n)$ as compared with the earlier ($U_{ext.}$ = 25 V) results. Namely, the slope of the linear $E_{mp}(n)$ relation (representing the strength of the VCCE effect) is nearly unaffected by the extraction voltages. It shows that the distortion of the VCCE effect by the extraction field is rather small and specifically, that the effect is getting more pronounced with decrease of the extraction voltage. The observation reported here is important for extending the range of validity of the VCCE effect and for gaining a deeper understanding of the nature and size of the (hypothesized) superhot moving precursor serving as the source for all the emitted clusters.

Introduction

Impact interactions of heavy atomic and polyatomic/cluster projectile ions with solid targets at the keV kinetic energy range play a central role in many fields and are interesting from both the fundamental and practical point of views. For example, the keV impact induced ejection of surface species (atomic and molecular) provide the basis for secondary ion mass spectrometry (SIMS) used for surface chemical mapping at submicronic resolution and for nanometrically resolved chemical depth profiling.[1,2] In the focused ion beams (FIB) technique, the erosion aspect of the sputtering event is used for surface patterning down to the few nm lateral scale.[3] Other applications and relevant processes include self – organized formation of periodic erosion pattern,[4,5] surface smoothing[6] and nanoscale damage to the outer surfaces of artificial[7] or natural[8] objects in space due to energetic collisions with nanograins and interstellar dust. Sputtering erosion of interstellar dust by high energy particles, in regions of dense dust clouds, is a major astrophysical process controlling the lifecycle of the dust grains and resulting star formation. In this context, it is interesting to mention that due to the recently established exceptional high abundance of C_{60} in the interstellar medium (up to 1% of all cosmic carbon),[9–12] sputtering erosion of dust grains by energetic C_{60} collisions may play a meaningful role in the interstellar medium (ISM). On the more fundamental level, there is an interest in characterizing (the poorly understood so far) sputtering mechanisms in energetic keV collisions between large polyatomic/cluster ions and solid targets[13–18] and especially, the puzzling emission of large secondary clusters, whose stability (at least for the duration of their flight time till detection) seems to contradict their highly energetic formation conditions. Impact of large atomic clusters with solid targets at the keV kinetic energy range can induce extreme energy densities at the few topmost layers of the sub-surface region manifested (within ~200 fs from impact) as extreme temperature and pressure spikes of a supercritical fluid.[19] This scenario requires that the constituent atoms (of the projectile cluster) will be lighter than target atoms. Atomically heavier clusters will penetrate the target lattice rather easily (clearing-the-way effect[13]) and energy deposition will not be as shallow as needed. Specifically, keV collision of a C_{60} projectile with metallic targets will result in such extreme conditions within a small sub-surface volume (the spike zone) containing up to

Schulich Faculty of Chemistry, Technion–Israel Institute of Technology, Haifa 3200003, Israel. E-mail: eliko@technion.ac.il

1000 atoms and only a few nm deep.[19] Such extreme conditions can give rise to a behavior which is very different from that observed when the impacting projectile ion is a heavy monoatomic one. Also, observables of the ultrafast (within the first ps from impact) secondary emission, such as kinetic energy distributions (KEDs) of a complete family of clusters of increasing size, emitted from a given target, carry important information reflecting the properties of this extreme state of matter before relaxing within the following few ps. Currently, these keV ion impact induced extreme conditions are not accessible experimentally by any other method. Assuming that the KEDs provide reliable diagnostics of the transient temperature and pressure of this unique state of matter one can potentially construct, combined with molecular dynamics (MD) based density calculations, an equation of states (EOS) for these extreme conditions. In this context we note that clusters emitted following the keV impact of a heavy monoatomic ion with a metallic target are assumed to originate from the rim of the impact crater at relatively late stage of the lifetime of the thermal spike (5–10 ps from impact) in an evaporation-like manner,[20–23] and therefore their KEDs carry very little information about the extreme sub-ps conditions of the spike. We note that this common assumption is based mainly on MD simulations since direct time resolved pump–probe measurements of keV ion impact induced dynamics below 100 ps are not yet available.

Recently, based on KEDs measurements of complete families of emitted clusters in collisions of keV C_{60}^- with different targets, we have reported a novel velocity correlated cluster emission (VCCE) effect.[19,24–27] The velocities of all outgoing cluster ions from each given target are correlated in the sense that they reflect a thermal distribution superimposed on a common center-of-mass velocity V_{CM}. This implies gradual shift of the KEDs to higher energies (as given by their most probable energy values $E_{mp}(n)$) and broadening with increase of cluster size n. The VCCE effect was measured for the metallic targets Au, Ag, Cu and Al (measuring KEDS of Au_n^+ (n = 1–15),[19] Ag_n^+ (n = 1–9),[24,26] Cu_n^+ (n = 1–9)[19,26] and Al_n^+ (n = 1–14)[25] cluster ions, respectively) and pre-grown thin carbidic films TaC and NbC (measuring KEDS of $Ta_nC_n^+$ (n = 1–10)[24,26] and $Nb_nC_n^+$ (n = 1–9)[26] cluster ions, respectively). The behavior of the KEDs of the emitted clusters following the C_{60}^- impact is very different (actually the opposite one) from that observed for the KEDs of both cationic and neutral clusters (sizes typically up to n = 7) emitted following surface impact of a heavy monoatomic ion (at the same energy), where the KEDs are getting narrower and shifted to lower energies with increase in cluster's size.[28–35]

Each complete family of measured KEDs of clusters emitted from a given target could be reproduced rather well within a model in which the source of the clusters is a superhot precursor moving with a center-of-mass velocity V_{CM} (in the lab coordinate system). This precursor state can be partially or fully detached from the surface.[24] The energy distributions of each complete family of emitted clusters of size n are therefore expressed by a shifted Maxwell function $f(E, n)$:

$$f(E,n) \propto E \cdot \exp\left[-\frac{\left(\sqrt{E}-\sqrt{n\varepsilon}\right)^2}{kT}\right], \qquad (1)$$

using a single pair of fitting parameters: the translational temperature T of the thermally distributed (in the precursor CM coordinate system) clusters and $\varepsilon = mV_{CM}^2/2$ which is the precursor translational energy per subunit. Here m is the mass of one atom for the homonuclear metallic clusters Me_n^+ with Me = Cu, Ag, Au, Al or mass of a single MeC subunit for the heteronuclear carbidic clusters $Me_nC_n^+$ with Me = Nb, Ta, and n as the number of units in the cluster.

A crucial aspect of the VCCE effect is the time window for the emission following a single C_{60}^- impact. In the absence of usable keV ion pulses (sufficiently intense, jitter free and synchronized) on the ps timescale, direct time resolved (pump–probe) measurements are not yet possible. This unfortunate situation implies that the intriguing time resolved dynamics of the thermal spike over the 0.1–20 ps timescale (evolution and decay) is experimentally inaccessible. This includes the dynamics of clusters emission by different mechanisms, energy transfer from the (collapsed) lattice to the electronic sub-system, *etc.* The VCCE effect is driven by the collisionally induced, exceptional high energy density produced in a relatively shallow subsurface region, at an early stage of the spike dynamics. We believe that the characteristics of the measured KEDS provide sufficient evidence (although indirect) showing that the correlated emission occurs within the first ps from impact, at the very early phase of the evolution of the thermal spike and well before formation of the crater. This is based on the velocity correlation effect itself, the high energies for emission (up to $E_{mp}(15)$ = 10.5 eV for the Ag_{15}^+ cluster[19] and the very high temperatures consistently derived from the Maxwellians fit (in the range of $kT \sim$ 1.1–1.3 eV). Also, detailed molecular dynamics (MD) calculations focusing on the sub-ps decay of the atomic number density within the spike nano volume support this conclusion.[19,26,27] In case that this decay is too fast to sustain the accumulation of a sufficiently high subsurface pressure as required for triggering the VCCE effect (efficiently propelling the precursor), we indeed measure a weakening of the effect (Al^{25}) down to its complete disappearance (Be^{27}). We have therefore concluded that the VCCE effect is at work within an ultra-short time window of only a few hundred fs, roughly extending between 200–500 fs from impact. The lower bound is dictated by the need for sufficient time for building up an intense pressure spike which is then decaying within the next few hundred fs. The KEDS of the emitted clusters therefore carry unique and valuable experimental information, not available so far, about the extreme conditions and state of matter existing within the first ps of keV ion-solid impact. Note that the ultra-short time scale for the clusters emission also implies that the translational temperature may not be fully equilibrated with the microcanonical internal (vibrational–rotational) temperature.

Using a simple thermodynamic model (the so-called piston mechanism)[19] based on the C_{60}^- impact induced isochoric heating of the subsurface nanovolume, followed by its adiabatic expansion, we have arrived at a simple relation expressing the accumulated sub-surface pressure P triggering the VCCE effect (movement of the precursor at V_{CM}) in terms of the experimental ε value. The model does not assume any specific equation of state (EOS) for the spike zone and resulted in the

relation $P = n_{prec.}\varepsilon$ with $n_{prec.}$ as the initial number density of the precursor. We assume $n_{prec.} \approx n_{crystal.}$ for the initial non-perturbed target based on the nature of the large clusters. Using this relation combined with the experimental ε value and MD based density calculations we arrive at an average pressure of 5 GPa for gold (over the 200–400 fs time window, from impact).[19]

The VCCE effect as measured for atomically heavy metallic target (Au, Ag, Cu) is fully developed for the emission of large clusters ($n > 5$), where the probability of other contributing mechanisms seems negligible. While for a gold target the VCCE effect is nicely obeyed for a relatively large cluster size range (n = 6–15),[19] the situation is less convincing for a silver target where measurements are limited to Ag_9^+. Here we extend the range of Ag_n^+ cluster sizes for which good quality KEDs are measured up to Ag_{21}^+ and show that the main characteristic of the correlated emission, a linear $E_{mp}(n)$ relation, remains valid even for the largest size range measured so far. This is achieved by using a higher extraction voltage than before, also demonstrating that the effect of the extraction voltage on the shape of the KEDs is rather minor.

Experimental

Here we provide some essential details of the experimental setup which is described in detail elsewhere.[19,26] The experimental configuration is presented in Fig. 1. A chemically cleaned polycrystalline Ag target was placed inside the UHV chamber and sputter annealed using 4 keV Ar^+ followed by up to 700 °C heating as done before.[36] It was then bombarded by 14 keV negatively charged C_{60}^- ions incident at 45° to the normal. The impact emitted positive Ag_n^+ cluster ions (n = 1–21) were collected along the normal using a 100 V extraction voltage into a quadrupole mass spectrometer (QMS – Extrel MEXM 4000) equipped with a homemade retarding field energy analyzer (RFA) allowing the measurement of highly mass resolved (1 amu) KEDs of all emitted cluster ions. The retarding electric field of the RFA is a uniform one, and its strength vectors are parallel to the normal (with respect to the target surface) and the axis of the RFA/QMS/detector assembly. Only axial velocity components are retarded, thus only ion kinetic energy corresponding to the normal component E_{nr} of the full kinetic energy E is being analyzed. However, as the half-angle of the aperture of the RFA/QMS/detector assembly is $\alpha \ll 1$, we assume (as before[19,24–26]) that $E \cong E_{nr}$. Sensitivity of the most probable energy values of the KEDs to the ion optical potentials (around maximum intensity) was found to be relatively small (implying sufficiently wide energy windows for ion transmission) and is covered by the given error bars. We also note that the shape of the KEDs is stable during the full measurement session (many hours) required for acquiring all the KEDs of the complete family of clusters. Namely, surface conditions over the rastered area are at steady state for the full measurement time.

The C_{60}^- ion beam was produced using a homemade capillary source.[19,26] The electron pickup process inside the capillary is very gentle resulting in fragmentation free C_{60}^- beam with mass purity of 99.9% or better. Kinetic energy spread is 0.55 eV or below (measurement limited). The beam is stable (below 2% drift per hour), intense (up to 80 nA at 10 keV) and quiet (current fluctuations below 0.1%). A complete description of the source along with its performance analysis will be published.[37] Performance of the C_{60}^- gun is superior to existing C_{60}^+ sources which are electron ionization based, and it is better suited for the KEDs measurements. During measurement, the beam was rastered over a 0.5 × 0.5 mm^2 area with a beam spot diameter of 30 μm and the target was kept at room temperature. The VCCE effect was also studied at elevated surface temperatures (up to 950 K for Nb target) but no change was found.[26] All applied potentials are accurate to within 0.1 volt or better as was also verified by measuring directly along the ion path by a precision digital multimeter. About 5–6 repeating KEDs measurements were averaged and smoothed for each cluster. A routinely used control and calibration measurement is that of the energy distribution of thermally emitted (surface ionized) K^+ which serves as a near-zero energy marker.

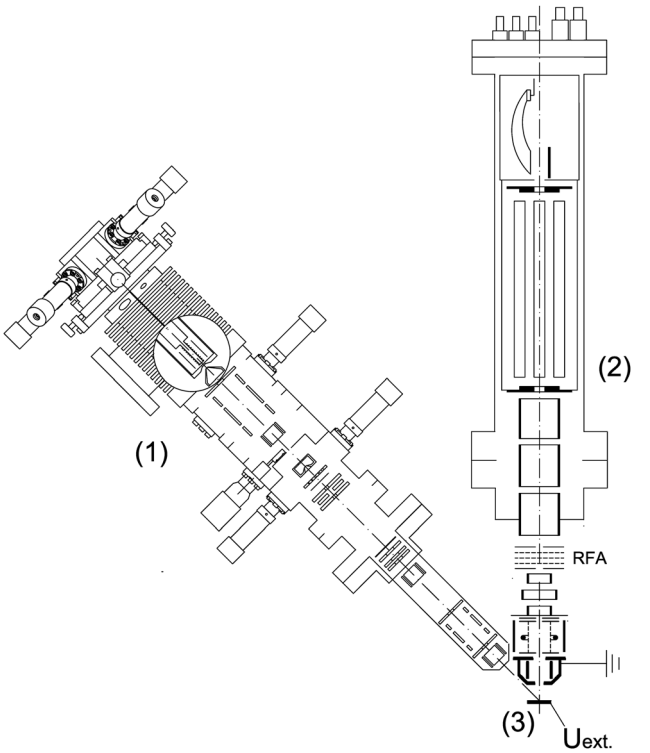

Fig. 1 Schematics of the experimental setup and extraction configuration (in bold) used for measuring the KEDS of the Ag_n^+ cluster ions emitted from an Ag target following impact of 14 keV C_{60}^- at 45° incidence. (1) C_{60}^- ion gun (source region including the heated capillary emitter + anode + extractor, is shown in the circularly exposed area) (2) RFA/QMS analyzer/detector assembly, (3) Ag target.

Results and discussion

The two main goals of the measurements as presented are: (1) to extend the range of cluster size for which the validity of the VCCE effect is tested. (2) To determine if the higher extraction voltage distorts in some way the observed characteristics of the

VCCE effect as measured earlier, and mainly the deduced strength of the VCCE effect. The strength of the VCCE effect for keV C_{60}^- impacting a specific target is determined by the value of ε derived from the measured KEDS. This value reflects the impact induced subsurface pressure driving the outward movement of the precursor and imparting a translational energy $\varepsilon = mV_{CM}^2/2$ to each of his subunits (single atoms for the case of metallic target). The pressure spike resulting in the measured ε value is an average over the few hundred fs time window effective for the correlated emission. A simple graphical representation of ε is given by the slope of the asymptotic form of the $E_{mp}(n)$ dependence as will be shown below. This dependence is obviously at work mainly for the larger cluster size range. Experimental $E_{mp}(n)$ dependences for large clusters are therefore a good way to compare ε values obtained under different impact or measurement conditions.

The ionization process of the metallic clusters emitted in the VCCE mode as induced by bombardment with keV C_{60}^- ions, is not well understood. Based on a simplified model of the formation of the VCCE effect (the ''piston'' model),[19] we believe that due to the extremely high temperature ($kT \sim 1$ eV) of the moving precursor (from which the detected cluster ions are emitted) some fraction of its constituent atoms and clusters are already in an ionized state. During the very early phase of the evolution of the thermal spike (within the 0.2–0.4 ps time-frame after C_{60}^- impact, well before formation of the crater), the nanovolume between these clusters (moving in the detector direction) and the undamaged part of the metal target contains atoms with a very high temperature and a greatly reduced averaged density (down to $\sim$0.5–0.4 of the density of the undamaged metal).[19,26] At such a low density, the energy structure of the electron system in this nanovolume should greatly differ from that of the undamaged metal and therefore hinders charge exchange between the metal and cluster ion (*e.g.*, its neutralization). A competing ionization channel *via* delayed thermionic emission (during flight) from a neutral Ag_n parent is highly unlikely, since the ionization energies of the neutral Ag_n clusters are considerably higher (by about 3–4 eV[38]) than the dissociation energies for the most favorable fragmentation channels: emission of a single neutral atom or a dimer. Note that calculated binding energy per atom for n = 2–13, 20 are about the same (1–3 eV) for both neutral and cationic clusters[39] approaching the bulk cohesive energy of 2.95 eV[40] for large clusters. Pronounced odd–even ion intensity alternations are observed here (14 keV C_{60}^- bombardment) favoring the odd-size cluster ions, similarly to that observed before for sputtered Ag_n^+ cluster ions using a heavy monoatomic projectile (10 keV Xe^+ (ref. 41)). The same behavior was also observed and studied in detail in collision induced dissociation (CID)[42,43] and photofragmentation measurements.[44] It was concluded that these odd–even intensity alternations reflect corresponding alternations in dissociation energies (measured to be in the range of 1–3 eV for n = 2–25[43]) resulting in preferential stability of the odd-size cluster ions (relative to the even-size ones) against delayed unimolecular (statistical) decay of the thermally excited ions, mainly *via* monomer evaporation.[42–44] We have therefore focused here on the higher intensity odd-numbered clusters. However, in order to get a more complete picture, given a sufficient signal we have also measured KEDs of even numbered clusters (n = 2, 4, 8, 14, 16).

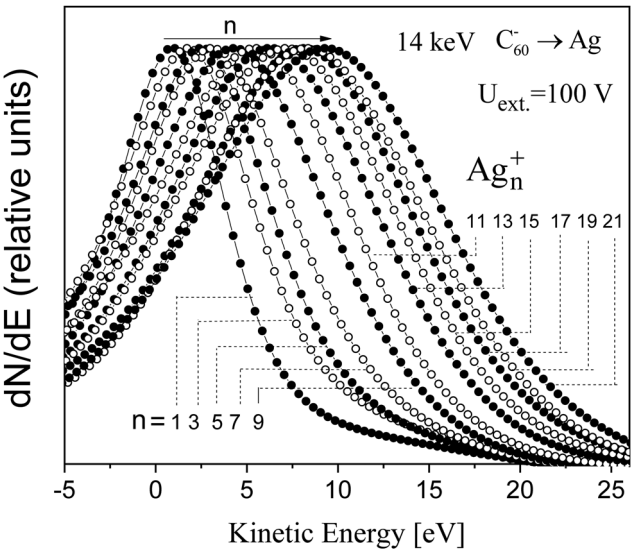

Fig. 2 Kinetic energy distributions (KEDs) of Ag_n^+ (n = 1, 3, 5, . . ., 21) cluster ions emitted from an Ag target following 14 keV impact of a C_{60}^- projectile ion at 45° incidence. Extraction volage is 100 V. All KEDs are normalized to the same value at their most probable energies. For the sake of clarity, only odd number cluster KEDs are shown. The presentation of the KEDs with alternating solid and empty circles only serves as a guide to eye.

Fig. 2 shows KEDs of odd numbered Ag_n^+ (n = 1, 3, 5, . . ., 21) clusters emitted from an Ag target following 14 keV impact of C_{60}^- projectile ion incident at 45°. Extraction of the cluster ions is along the normal at 100 V. For the sake of clarity, measured KEDs of even numbered Ag_n^+ clusters were omitted and the KEDS in the figure are shown with alternating solid and empty circles. The main features of the KEDs are in line with the earlier measurements of Ag_n^+ (n = 1–9),[24,26] namely, gradual shift of the KEDs to higher energies and broadening with increase of cluster size. Extending the range of measured KEDs from the former (n = 1–9) up to n = 21 here was made possible by several improvements in signal to noise ratio but mainly by the higher extraction voltage of 100 V as compared with 25 V before,[24,26] thus enabling better collection of ions emitted at off-normal angles. We did not attempt to fit the KEDs with a shifted Maxwellian energy distribution as done for all the former cluster correlated emission measurements (for the purpose of extracting ε and kT). The mixing/superimposing of mainly normally emitted clusters with a preferentially large fraction of off-normal low energy (field bent) trajectories can potentially bias the fitting process and reduce its reliability. Already when visually comparing the present KEDs (100 V) with the former ones (25 V) one can see that the low energy tail is indeed more pronounced now, in line with the field induced enrichment in low energy trajectories. In early studies the weak field 25 V extraction was chosen as a compromise between minimal field induced distortion (mainly on the very low energy side) and good signal to noise ratio enabling the measurement

of high quality KEDS of large clusters. The present results support this choice.

Fig. 3 shows the most probable energy values of all measured KEDS from both the earlier measurements ($U_{ext.}$ = 25 V, empty circles)[24,26] and the present measurements ($U_{ext.}$ = 100 V, solid triangles), denoted $E_{mp}(n, 25\ V)$ and $E_{mp}(n, 100\ V)$ correspondingly. The error bars are ± one standard deviation over 5–6 independent repeating measurements. In the earlier $U_{ext.}$ = 25 V measurements, the complete family of KEDs was fitted by shifted Maxwellians (eqn (1)) according with the precursor model resulting in ε = 0.40 eV and kT = 1.13 eV as a single pair of fitting parameters reproducing the experiment reasonably well. The solid line is given by (connecting) the most probable energies $E_{mp}(n)$ for the shifted Maxwellian

$$E_{mp}(n) = \frac{n\cdot\varepsilon}{4}\cdot\left(1+\sqrt{1+\frac{4kT}{n\cdot\varepsilon}}\right)^2, \quad (2)$$

and the dashed line is describing the oblique asymptote for large values of n ($n\cdot\varepsilon \gg 4kT$) as given by

$$E_{mp}(n) = n\cdot\varepsilon + 2kT. \quad (3)$$

Both relations are plotted using the experimentally derived (fitted) ε, kT values as given above. Although the cluster size n is a discrete variable, for the sake of clarity we treat it here as a continuous one. Especially for the asymptotic expression eqn (3), it is convenient for extracting ε value as the slope and the kT value from the y-intercept. Note that $E_{mp}(n)$ values derived from both expressions are quite similar already from n = 7 (and for other targets such as NbC and TaC even for smaller clusters[24,26]). Eqn (3) is interesting since it presents

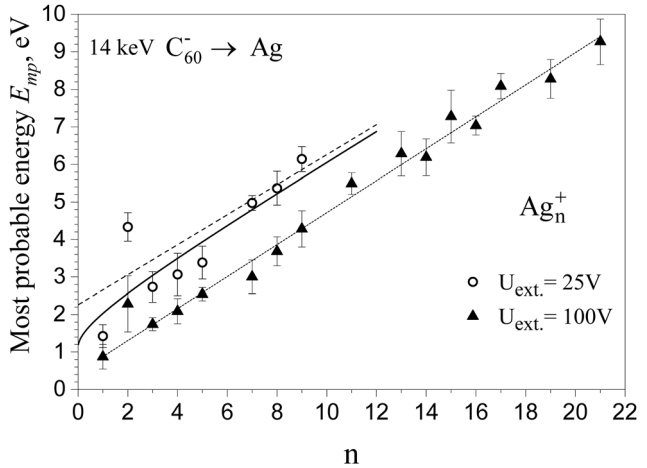

Fig. 3 Most probable kinetic energies of emitted Ag_n^+ cluster ions ($E_{mp}(n)$) following 14 keV impact of a C_{60}^- projectile ion with an Ag target at a 45° incidence. Shown are measured values for 25 V and 100 V extraction voltages. The $E_{mp}(n, 25\ V)$ values (empty circles) are taken from ref. 24 along with calculated values (thick solid line and dashed line) based on a shifted Maxwellian for the KEDs (moving thermal precursor model, see text). The $E_{mp}(n, 100\ V)$ values (solid triangles) are taken from Fig. 1 along with additional even numbered KEDs up to Ag_{21}^+. The dense dashed line is a best fit to the measured values.

$E_{mp}(n)$ (in the limit of large n) as a sum of two independent kinetic energy terms. The $n\cdot\varepsilon$ term is associated with the CM movement of the precursor (V_{CM}) and the $2kT$ term is associated with the thermal motion in the CM frame. This separability is useful as it provides a good approximation for large values of n.

The observations obtained from the $E_{mp}(n, 100\ V)$ measurements can be summarized as follows: (1) a nearly linear dependence is observed, in line with the precursor model predictions (eqn (2) and (3)). The dense dashed line is a best fit to the measured $E_{mp}(n, 100\ V)$ values. (2) The slope of this nearly linear dependence is about the same as that of the $E_{mp}(n, 25\ V)$ dependence (especially above n = 4), this implies that the ε value (see eqn (3)) is nearly the same for both dependences (at least as determined by $E_{mp}(n)$ values only). (3) The increased collection and detection of the off-normal lower energy cluster ions by the 100 V extraction resulted in a rather moderate and nearly constant 1–2 eV decrease of $E_{mp}(n, 100\ V)$ values as compared with the earlier $E_{mp}(n, 25\ V)$ results. (4) The E_{mp} value of the Ag_2^+ dimer is exceptionally high in both the 25 V and 100 V measurements. The ratio of dimer to monomer E_{mp} values is about 3 for the earlier 25 V measurement and about 2.6 for the present 100 V measurements. We tentatively attribute this behavior to the contribution of an additional mechanism, which is at work mainly for the dimers. A plausible formation mechanism for the Ag_2^+ dimer is a recombination between two independently emitted atoms moving with a mutual velocity mismatch corresponding to CM kinetic energy below the dimer dissociation energy.[45] Such a mechanism usually requires the two-body association to occur very close to the surface, still within the range of the surface potential, in order to stabilize the dimer by draining excess vibrational energy. Interestingly, this irregularly high E_{mp} value of the emitted dimer ion is observed for all three coin metals[26] but is most pronounced for Ag. This behavior is different than that observed for emitted carbidic clusters from ultrathin NbC and TaC layers[24,26] where the dimers E_{mp} values obey the linear dependence as in eqn (3).

The conclusions derived from these observations are as follows: (1) the VCCE effect as an outcome of the precursor mechanism and as described by shifted Maxwellian KEDs is shown to be valid till Ag_{21}^+. This is a meaningful extension of the validity range beyond the former rather limited range of up to Ag_9^+. This is also the largest range of correlated cluster emission ever observed for any target beyond Au_{15}^+ and Al_{14}^+ as measured for 14 keV C_{60}^- impact with gold[19] and aluminum[25] targets respectively. We note that large cluster emissions are especially important for demonstrating the VCCE effect. (2) Increasing the extraction voltage leads to increased signal by collecting a larger fraction of clusters emitted at off-normal angles (by bending their initial outgoing trajectories). These clusters are preferentially of lower energy (with respect to the normally emitted ones) resulting in $E_{mp}(n, 100\ V)$ values somewhat lower than the $E_{mp}(n, 25\ V)$ values. (3) The effect caused by the fraction of off-normal low energy clusters collected by the 100 V extraction is rather similar for all cluster sizes (within error bars) and therefore the down shift of all

$E_{mp}(n, 100\ V)$ values to lower energies is about the same and the slope of the linear dependence (ε value, reflecting the strength of the VCCE effect) is similar to that exhibited by the $E_{mp}(n, 25\ V)$ dependence. This fraction is relatively modest as an increase of the extraction voltage by a factor of 4 results in a down shift of $E_{mp}(n)$ values by only 1–2 eV.

We have already emphasized the importance of extending the clusters size range of KEDs measurements since the VCCE effect is best manifested for the large clusters where possible contributions by other statistical mechanisms are negligible. Also, since the clusters originate from the superhot moving precursor, their maximal size provide information about the nature and size of the precursor. An additional reason to focus on the large clusters is related with the fact that due to their high translational temperatures ($kT \sim 1$ eV), the most probable velocities V_{mp} of the relatively small (up to n = 4–7 per target) emitted clusters are actually strongly mass dependent, approaching asymptotically the precursor velocity V_{CM} for large clusters.[26] The shifted Maxwell velocity distribution is given by $\frac{dN_n}{dV} \propto V^3 \exp\left[-\frac{nm(V-V_{CM})^2}{2k_BT}\right]$ with $V_{mp}(n) = (V_{CM}/2)\cdot\left[1+\sqrt{1+(6kT/n\varepsilon)}\right]$ and $\varepsilon = mV_{CM}^2/2$. Recall (see Experimental) that within this presentation both V and V_{CM} are nearly parallel and axially directed along the surface normal and the RFA/QMS axis. The extended range as measured here describes the gradual approach of the V_{mp} value of the large Ag_n^+ clusters to the common precursor velocity. The behavior of large clusters according to the precursor model also emphasizes the fact that an alternative model of gas dynamic acceleration in adiabatic free jet like expansion (seeded beam) cannot properly describe the results. Here we measure an asymptotical convergence of the clusters V_{mp} values to a final velocity (V_{CM}) with increasing cluster size, while seeded beams are characterized by a velocity mismatch (cluster velocity *vs.* terminal flow velocity) which is increasing with the mass of the seed species (velocity slip effect).[46–49] We also note that the axial velocity distribution usually assumed in free jet expansion[49–51] (neglecting perpendicular velocity components) is similar to the shifted Maxwell distribution as given above (for the precursor model) with similar V_{mp} expression, but with terminal flow velocity instead of the precursor CM velocity (drifting Maxwellian distribution). This implies that similarly to the case of the precursor mechanism and due to the high temperatures involved, also within a free jet model the small clusters range will not show any velocity (V_{mp}) uniformity but a strong mass dependence.

Summary

We have measured kinetic energy distributions (KEDs) of positive cluster ions Ag_n^+ emitted from a clean silver target following impact of 14 keV C_{60}^-. The measurements cover the range n = 1–21 thus extending former measurements which were limited to the n = 1–9 range. We have found that all the clusters in the extended range up to Ag_{21}^+ are emitted in a velocity correlated fashion. This is the largest range of emitted clusters observed so far to obey the VCCE effect. Accessing the high size range is especially important since the VCCE effect is expected to be better manifested for large clusters whose velocity is asymptotically approaching the precursor CM velocity. The present measurements are made possible mainly by increasing the ion extraction voltage to 100 V, preferentially collecting some off-normal low energy cluster ions. It is found that the dependence of the KEDs most probable energies on cluster size behaves nearly linearly with a slope which is about the same as that observed in earlier measurements with an extraction voltage of 25 V, thus corresponding (as it should) to the same strength of the VCCE effect. The KEDS measured with the higher extraction voltage are found to be only moderately shifted (by 1–2 eV) to lower energies as compared with the KEDs measured before with the lower extraction voltage. Namely, the VCCE effect is getting more pronounced with decrease of the extraction field.

Conflicts of interest

There are no conflicts to declare.

Data availability

The paper reports on a direct measurement of kinetic energy distributions (KEDs) of impact emitted Ag_n^+ (n = 1–21) clusters and therefore the measured basic data (the KEDs) is reported and is available in the paper itself (see Fig. 2). Fig. 3 shows the most probable energies of the KEDs (maximum intensity peaks) taken directly from Fig. 2 as a function of cluster size. This is again directly measured data.

References

1 A. Benninghoven, F. G. Rudenauer and H. W. Werner, *Secondary Ion Mass Spectrometry, Basic Concepts, Instrumental Aspects, Applications and Trends*, Wiley-InterScience Publications, 1987.
2 *ToF-SIMS: Surface Analysis by Mass Spectrometry*, ed. J. C. Vickerman and D. Briggs, IM Publications and Surface Spectra Limited, Chichester, UK, 2001.
3 *Focused Ion Beam Systems: Basic and Applications*, ed. N. Yao, Cambridge University Press, 2007.
4 R. M. Bradley and P. D. Shipman, *Phys. Rev. Lett.*, 2010, **105**, 145501.
5 P. Karmakar, G. F. Liu, Z. Sroubek and J. A. Yarmoff, *Phys. Rev. Lett.*, 2007, **98**, 215502.
6 N. Toyoda, N. Hagiwara, J. Matsuo and I. Yamada, *Nucl. Instrum. Methods Phys. Res., Sect. B*, 2000, **161**, 980.
7 F. Hörz, R. Bastien, J. Borg, J. P. Bradley, J. C. Bridges, D. E. Brownlee, M. J. Burchell, M. Chi, M. J. Cintala, Z. R. Dai, Z. Djouadi, G. Dominguez, T. E. Economou, S. A. J. Fairey, C. Floss, I. A. Franchi, G. A. Graham, S. F. Green, P. Heck, P. Hoppe, J. Huth, H. Ishii, A. T. Kearsley, J. Kissel, J. Leitner, H. Leroux, K. Marhas,

K. Messenger, C. S. Schwandt, T. H. See, C. Snead, F. J. Stadermann I, T. Stephan, R. Stroud, N. Teslich, J. M. Trigo-Rodríguez, A. J. Tuzzolino, D. Troadec, P. Tsou, J. Warren, A. Westphal, P. Wozniakiewicz, I. Wright and E. Zinner, *Science*, 2006, **314**, 1716.
8 R. E. Johnson, *Energetic Charged-Particle Interactions with Atmospheres and Surfaces*, Springer, Berlin, 1990.
9 J. P. Maier and E. K. Campbell, *Angew. Chem., Int. Ed.*, 2017, **56**, 4920.
10 E. K. Campbell, M. Holz, D. Gerlich and J. P. Maier, *Nature*, 2015, **523**, 322.
11 J. Cami, J. Bernard-Salas, E. Peeters and S. E. Malek, *Science*, 2010, **329**, 1180.
12 B. H. Foing and P. Ehrenfreund, *Nature*, 1994, **369**, 296.
13 V. N. Popok, I. Barke, E. E. B. Campbell and K.-H. Meiwes-Broer, *Surf. Sci. Rep.*, 2011, **66**, 347.
14 V. N. Popok and E. E. B. Campbell, *Rev. Adv. Mater. Sci.*, 2006, **11**, 19.
15 Z. Postawa, B. Czerwinski, M. Szewczyk, E. J. Smiley, N. Winograd and B. J. Garrison, *J. Phys. Chem. B*, 2004, **108**, 7831.
16 S. F. Belykh, U. Kh Rasulev, A. V. Samartsev and I. V. Veryovkin, *Nucl. Instrum. Methods Phys. Res., Sect. B*, 1998, **136–138**, 773.
17 S. F. Belykh, B. Habets, U. K. Rasulev, A. V. Samartsev, L. V. Stroev and I. V. Veryovkin, *Nucl. Instrum. Methods Phys. Res., Sect. B*, 2000, **164–165**, 809.
18 S. Sun, C. Szakal, N. Winograd and A. Wucher, *J. Am. Soc. Mass Spectrom.*, 2005, **16**, 1677.
19 E. Armon, E. Zemel, A. Bekkerman, V. Bernstein, B. Tsipinyuk and E. Kolodney, *J. Chem. Phys.*, 2019, **150**, 204705.
20 M. Urbassek, in *Sputtering by Particle Bombardment. Topics in Applied Physics 110*, ed. R. Behrisch and W. Eckstein, Springer-Verlag, Berlin, Heidelberg, 2007, p. 189.
21 G. Betz and W. Husinsky, *Philos. Trans. R. Soc., A*, 2004, **362**, 177.
22 K. Nordlund, J. Keinonen, M. Ghaly and R. S. Averback, *Nucl. Instrum. Methods Phys. Res., Sect. B*, 1999, **148**, 74.
23 T. J. Colla, R. Aderjan, R. Kissel and H. M. Urbassek, *Phys. Rev. B:Condens. Matter Mater. Phys.*, 2000, **62**, 8487.
24 E. Armon, A. Bekkerman, Y. Cohen, J. Bernstein, B. Tsipinyuk and E. Kolodney, *Phys. Rev. Lett.*, 2014, **113**, 027604.
25 A. Bekkerman, B. Tsipinyuk and E. Kolodney, *Nucl. Instrum. Methods Phys. Res., Sect. B*, 2020, **481**, 24.
26 E. Armon, A. Bekkerman, V. Bernstein, B. Tsipinyuk and E. Kolodney, *Phys. Chem. Chem. Phys.*, 2022, **24**, 19634.
27 V. Bernstein, A. Bekkerman and E. Kolodney, *J. Chem. Phys.*, 2024, **160**, 054705.
28 (*a*) I. V. Veryovkin, S. F. Belykh, A. Adriaens and F. Adams, *Nucl. Instrum. Methods Phys. Res., Sect. B*, 2004, **219–220**, 215; (*b*) I. V. Veryovkin, S. F. Belykh, A. Adriaens, A. V. Zinovev and F. Adams, *Appl. Surf. Sci.*, 2004, **231–232**, 101.
29 G. Betz and K. Wien, *Int. J. Mass Spectrom. Ion Processes*, 1994, **140**, 1.
30 H. Gnaser, in *Sputtering by Particle Bombardment. Topics in Applied Physics 110*, ed. R. Behrisch and W. Eckstein, Springer-Verlag, Berlin, Heidelberg, 2007, p. 231.
31 Z. Ma, W. F. Calaway, M. J. Pellin and E. I. von Nagy-Felsobuki, *Nucl. Instrum. Methods Phys. Res., Sect. B*, 1994, **94**, 197.
32 S. R. Coon, W. F. Calaway, M. J. Pellin and J. M. White, *Surf. Sci.*, 1993, **298**, 161.
33 S. R. Coon, W. F. Calaway, M. J. Pellin, G. A. Curlee and J. M. White, *Nucl. Instrum. Methods Phys. Res., Sect. B*, 1993, **82**, 329.
34 M. Wahl and A. Wucher, *Nucl. Instrum. Methods Phys. Res., Sect. B*, 1994, **94**, 36.
35 C. Staudt and A. Wucher, *Phys. Rev. B:Condens. Matter Mater. Phys.*, 2002, **66**, 075419.
36 Y. Cohen, V. Bernstein, E. Armon, A. Bekkerman and E. Kolodney, *J. Chem. Phys.*, 2011, **134**, 124701.
37 A. Bekkerman, B. Tsipinyuk and E. Kolodney, *to be submitted*.
38 C. Jackschath, I. Rabin and W. Schulze, *Z. Phys. D:At., Mol. Clusters*, 1992, **22**, 517–520.
39 E. M. Fernández, J. M. Soler, I. L. Garzón and L. C. Balbás, *Phys. Rev. B:Condens. Matter Mater. Phys.*, 2004, **70**, 165403.
40 C. Kittel. *Introduction to Solid State Physics*, John Wiley & Sons, Inc, Hoboken, NJ, 8th edn, 2005.
41 I. Katakuse, T. Ichihara, Y. Fujita, T. Matsuo, T. Sakurai and H. Matsuda, *Int. J. Mass Spectrum Ion Processes*, 1985, **67**, 229–236.
42 S. Krückeberg, G. Dietrich, K. Lutzenkirchen, L. Schweikhard, C. Walter and J. Ziegler, *Int. J. Mass Spectrum Ion Processes*, 1996, **155**, 141–148.
43 S. Krückeberg, G. Dietrich, K. Lutzenkirchen, L. Schweikhard, C. Walter and J. Ziegler, *J. Chem. Phys.*, 1999, **110**, 7216.44.
44 U. Hild, G. Dietrich, S. Krückeberg, M. Lindinger, K. Lützenkirchen, L. Schweikhard, C. Walther and J. Ziegler, *Phys. Rev. A:At., Mol., Opt. Phys.*, 1998, **57**, 2786–2793.
45 Y. Cohen and E. Kolodney, *Nucl. Instrum. Methods Phys. Res., Sect. B*, 2011, **269**, 985.
46 D. R. Miller, Free Jet Sources, in *Atomic and Molecular Beam Methods*, ed. G. Scoles, Oxford University Press, New York, 1988, p. 14.
47 E. Kolodney and A. Amirav, *Chem. Phys.*, 1983, **82**, 269.
48 B. Tsipinyuk, A. Budrevich and E. Kolodney, *J. Phys. Chem.*, 1996, **100**, 1475.
49 H. Pauli, *Atom, molecule and cluster beam I and II*, Springer-Verlag, Berlin-Heidelberg, 2000.
50 A. Kantrowitz and J. Grey, *Rev. Sci. Instrum.*, 1951, **22**, 328.
51 D. P. Woodruff and T. A. Delchar, *Modern Techniques of Surface Science*, Cambridge University Press, 1986.